View metadata, citation and similar papers at core.ac.uk

brought to you by CORE

provided by Elsevier - Publisher Connector

Available online at www.sciencedirect.com

ScienceDirect

Polar Science 4 (2011) 550–557

NiPR National Institute of Polar Research

http://ees.elsevier.com/polar/

Petrography of Yamato 984028 lherzolitic shergottite and its melt vein: Implications for its shock metamorphism and origin of the vein

Shin Ozawa [a,*], Masaaki Miyahara [a], Eiji Ohtani [a], Makoto Kimura [b], Yoshinori Ito [a]

[a] *Department of Earth and Planetary Materials Science, Graduate School of Science, Tohoku University, Sendai 980-8578, Japan*
[b] *Faculty of Science, Ibaraki University, Mito 310-8512, Japan*

Received 15 October 2009; revised 3 May 2010; accepted 27 August 2010
Available online 22 September 2010

Abstract

Yamato 984028 (Y984028) is a newly identified lherzolitic shergottite, recovered from the Yamato Mountains, Antarctica, in 1999. As part of a consortium study, we conducted petrographic observations of Y984028 and its melt vein in order to investigate its shock metamorphism. The rock displays the typical non-poikilitic texture of lherzolitic shergottite, characterized by a framework of olivine, minor pyroxene (pigeonite and augite), and interstitial maskelynite. Shock metamorphic features include irregular fractures in olivine and pyroxene, shock-induced twin-lamellae in pyroxene, and the complete conversion of plagioclase to maskelynite, features consistent with those found in other lherzolitic shergottites. The melt vein is composed of coarse mineral fragments (mainly olivine) entrained in a matrix of fine-grained euhedral olivine (with several modes of compositional zoning) and interstitial glassy material. Some coarse olivine fragments consist of an assemblage of fine-grained euhedral to subhedral olivine crystals, suggesting shock-induced fragmentation, recrystallization, and/or a process of sintering. The implication is that the fine-grained olivine crystals in the matrix of the melt vein represent complicated crystallization environments and histories.
© 2010 Elsevier B.V. and NIPR. All rights reserved.

Keywords: Martian meteorites; Shock metamorphism; Melt vein; Chemical zoning; Sintering

1. Introduction

It is widely accepted that SNC (Shergottites–Nakhlites–Chassignites) meteorites are derived from Mars (e.g., Bogard and Johnson, 1983; McSween, 1994; Marti et al., 1995; Clayton and Mayeda, 1996). As we have not yet recovered any samples directly from Mars, Martian meteorites are the only materials available for investigating the nature and history of Mars. Among the currently recognized 83 Martian meteorites, shergottite is the largest group with 69 members. Shergottites are basaltic to lherzolitic igneous rocks, probably formed near the surface of Mars (e.g., McSween and Treiman, 1998; Nyquist et al., 2001), and an investigation of them is therefore especially important for understanding Martian igneous activity.

Shergottites are characterized by a high degree of shock metamorphism (e.g., McSween and Treiman, 1998; Nyquist et al., 2001) typified by shock-induced melt veins and melt pockets. For instance, akimotoite, a high-pressure polymorph of pyroxene, was reported in thin melt veins of the lherzolitic shergottite Y000047 (Mikouchi and Kurihara, 2008; Imae and Ikeda, 2010). The shock metamorphic features and high-pressure

* Corresponding author. Tel.: +81 22 795 6664; fax: +81 22 795 6662.
E-mail address: shin-ozawa@m.tains.tohoku.ac.jp (S. Ozawa).

1873-9652/$ - see front matter © 2010 Elsevier B.V. and NIPR. All rights reserved.
doi:10.1016/j.polar.2010.08.002

phases in Martian meteorites provide crucial information about the nature and history of impact events on Mars (e.g., El Goresy, 2009; Akaogi et al., 2010).

Yamato 984028, hereafter referred to as Y984028, is a newly identified lherzolitic shergottite, found in 1999 in the Yamato Mountains, Antarctica. Our study of Y984028 is part of a consortium study organized by the National Institute of Polar Research (NIPR), Japan. The main object of this work was to investigate shock metamorphic features in the meteorite, and here we present the preliminary results of our petrographic investigation of the rock and its melt vein.

2. Sample and experimental methods

We obtained a chip sample of Y984028 from NIPR. The sample is granular with a greenish or yellowish color. A wide black vein can be seen at the center of the chip. The sample was embedded in resin, then cut across the vein. A cut chip sample was then attached to a glass slide using a crystal bond, and polished with an abrasive.

We examined the polished sample in the following ways. Textural observations were made with a JEOL JSM-71010 field-emission gun scanning electron microscope (FEG-SEM) at an accelerating voltage of 15 kV. The chemical compositions of minerals and glass were determined with a JEOL JXA8800M electron probe micro-analyzer (EPMA) equipped with a wavelength dispersive X-ray spectrometer (WDS). The accelerating voltage and electron beam current were 15 kV and 5–15 nA, respectively, and the beam diameter was 1–10 μm. Standard materials used were as follows: synthetic forsterite (Mg_2SiO_4) for Si and Mg, synthetic TiO_2 for Ti, synthetic corundum (Al_2O_3) for Al, synthetic Cr_2O_3 for Cr, synthetic fayalite (Fe_2SiO_4) for Fe, synthetic Mn_2SiO_4 for Mn, natural wollastonite ($CaSiO_3$) for Ca, natural jadeite ($NaAlSi_2O_6$) for Na, natural adularia ($KAlSi_3O_8$) for K, and synthetic NiO for Ni. Phase identifications of the minerals and glass were conducted with a JASCO NRS-2000 laser micro-Raman spectrometer (Ar + laser, 514.5 nm line). The laser power was 8–20 mW, and the laser beam was ~1 μm in diameter. The Raman spectra were collected for a period of 60–120 s, and accumulated twice.

3. Results

3.1. Petrography of the shergottite that hosts the melt vein

A back-scattered electron (BSE) image of the sample is shown in Fig. 1. The major constituent minerals in the

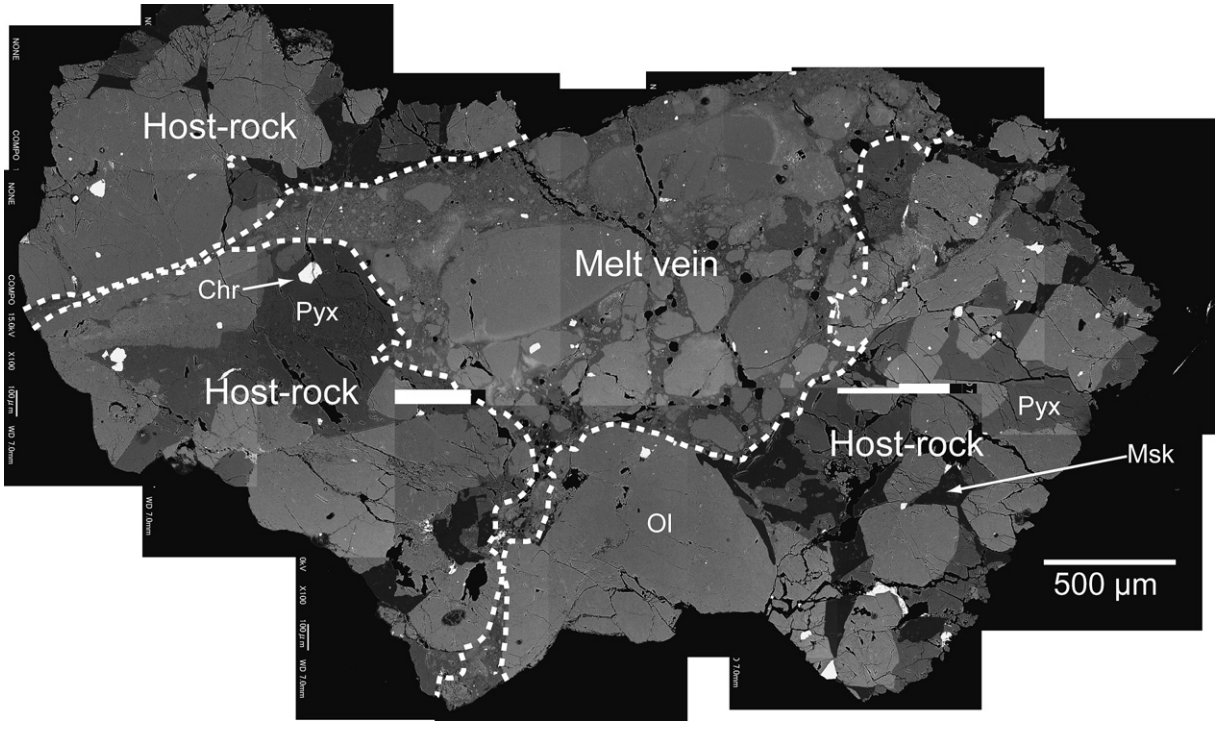

Fig. 1. Back-scattered electron image of the entire lherzolitic shergottite specimen Y984028. The specimen consists of host shergottite with a melt vein up to 1.5 mm wide. Ol = olivine; Pyx = pyroxene; Msk = maskelynite; Chr = chromite.

shergottite are olivine (Fo_{67-69}), augite ($En_{51-55}Fs_{16-17}Wo_{29-34}$), pigeonite ($En_{64-67}Fs_{23-27}Wo_{7-11}$), maskelynite ($Ab_{44-54}An_{44-54}Or_{1-2}$), and chromite (Table 1).

Euhedral to subhedral olivine (0.2−1.0 mm in diameter) is the most abundant phase, and the crystals contain numerous irregular fractures. Augite and pigeonite (0.2−1.0 mm in diameter) are the next most abundant phases, and their subhedral to anhedral crystals are found in the interstices of the olivine grains. Augite usually seems to exist at the grain margins of pigeonite. Many irregular fractures are also observed in the augite and pigeonite grains. Shock-induced twin-lamellae are found in some pyroxene grains. Maskelynite (100−500 μm in

Table 1
Chemical compositions of the constituent minerals and glass in Y984028 lherzolitic shergottite.

	Olivine[a]		Augite[a]		Pigeonite[a]		Maskelynite[a]		Chromite[b] (core)	Chromite[b] (rim)
n	14		4		6		7		1	1
Chemical composition (wt%)										
	av.	s.d.	av.	s.d.	av.	s.d.	av.	s.d.		
SiO_2	37.14	0.22	52.57	0.63	53.91	0.53	54.36	0.80	b.d.	b.d.
TiO_2	b.d.	−	0.31	0.11	0.35	0.22	n.d.	−	1.11	1.70
Al_2O_3	b.d.	−	1.50	0.47	0.84	0.22	26.94	0.99	6.76	8.30
Cr_2O_3	n.d.	−	0.72	0.05	0.36	0.12	n.d.	−	58.07	55.34
V_2O_3	n.d.	−	n.d.	−	n.d.	−	n.d.	−	0.62	0.65
Fe_2O_3	−	−	−	−	−	−	−	−	2.45	3.15
FeO	28.84	0.38	10.07	0.51	16.53	1.00	0.55	0.17	26.35	26.58
MnO	0.61	0.05	0.43	0.03	0.64	0.06	n.d.	−	0.43	0.51
NiO	b.d.	−	n.d.	−	n.d.	−	n.d.	−	n.d.	n.d.
MgO	34.18	0.50	18.29	0.90	23.75	0.52	n.d.	−	4.95	5.44
ZnO	n.d.	−	n.d.	−	n.d.	−	n.d.	−	b.d.	b.d.
CaO	0.18	0.04	14.83	0.86	4.38	0.75	9.90	0.71	b.d.	b.d.
Na_2O	n.d.	−	0.22	0.01	0.07	0.01	5.30	0.45	n.d.	n.d.
K_2O	n.d.	−	b.d.	−	b.d.	−	0.27	0.05	n.d.	n.d.
Total	100.95	0.79	98.95	0.50	100.83	0.46	97.31	0.73	100.73	101.66
Cation formula										
Si	0.990	0.005	1.956	0.013	1.963	0.007	2.518	0.039	−	−
Ti	−	−	0.009	0.003	0.010	0.006	−	−	0.029	0.043
Al	−	−	0.066	0.021	0.036	0.009	1.471	0.048	0.275	0.332
Cr	−	−	0.021	0.002	0.010	0.003	−	−	1.586	1.484
V	−	−	−	−	−	−	−	−	0.017	0.018
Fe^{3+}	−	−	−	−	−	−	−	−	0.064	0.080
Fe^{2+}	0.643	0.008	0.313	0.015	0.503	0.032	0.021	0.006	0.761	0.754
Mn	0.014	0.001	0.014	0.001	0.020	0.002	−	−	0.013	0.015
Ni	−	−	−	−	−	−	−	−	−	−
Mg	1.358	0.011	1.014	0.043	1.289	0.020	−	−	0.255	0.275
Zn	−	−	−	−	−	−	−	−	−	−
Ca	0.005	0.001	0.591	0.038	0.171	0.030	0.491	0.035	−	−
Na	−	−	0.016	0.001	0.005	0.001	0.476	0.042	−	−
K	−	−	−	−	−	−	0.016	0.003	−	−
Total	3.010	0.005	4.000	0.004	4.007	0.002	4.993	0.011	3.000	3.000
Oxygen	4		6		6		8		4	4
Molecular proportions										
Fo	68	<1	En	53	2	66	1	Ab	48	4
Fa	32	<1	Fs	16	1	26	2	An	50	4
			Wo	31	2	9	2	Or	2	<1

Key: *n* = number of analyses; av. = average chemical composition; s.d. = standard deviation of analyses (1σ); b.d. = below the detection limit; n.d. = not determined.
Detection limits (in wt%): $TiO_2 = 0.02$, $Al_2O_3 = 0.02$, and NiO = 0.07 for olivine; $K_2O = 0.01$ for augite and pigeonite; $SiO_2 = 0.04$, ZnO = 0.08, and CaO = 0.02 for chromite.
[a] All iron is assumed to be ferrous.
[b] All iron was analyzed as ferrous iron, and recalculated to determine the content of ferric iron using the method proposed by Droop (1987).

diameter) exists as subhedral to anhedral grains in the interstices of the olivines and/or pyroxenes. There are only a few fractures in most of the maskelynite. Chromite (10–100 μm in diameter) exists as euhedral crystals, mostly enclosed within olivine or pyroxene. Some chromite grains have compositional zoning, with Cr-rich cores and Ti-, Al-, and Fe-rich rims (Table 1).

3.2. Petrography of the melt vein

A melt vein up to 1.5 mm wide occurs at the center of the sample (Fig. 1), and it consists of coarse mineral fragments entrained in a matrix. The fragments are mainly olivine (Fo_{68-70}) (Fig. 2 and Table 2) with minor pigeonite ($En_{61-65}Fs_{26-27}Wo_{8-14}$), maskelynite ($Ab_{54-62}An_{36-45}Or_{1-2}$), and chromite (Table 2).

Olivine fragments in the melt vein have rounded shapes and fewer fractures than the olivine in the host shergottite (Fig. 2a). Some fragments are a polycrystalline assemblage of fine-grained euhedral to subhedral olivine (Fig. 2b–c). In some cases, only the margins of fragments, adjacent to the melt vein matrix, display this polycrystalline texture. The polycrystalline margins are enriched in Al and Ca, probably reflecting a contribution from the matrix glass between the olivine crystals. In addition, tiny bright crystals, probably chromite, are found in the interstices of the olivine crystals.

Pigeonite fragments in the melt vein also have rounded shapes, and they may also partially show a polycrystalline texture. There are fewer fractures in the pigeonite fragments of the melt vein than in those of the host shergottite. Maskelynite fragments in the melt vein have rounded irregular shapes, and our identification of these as amorphous fragments is supported by the Raman spectra.

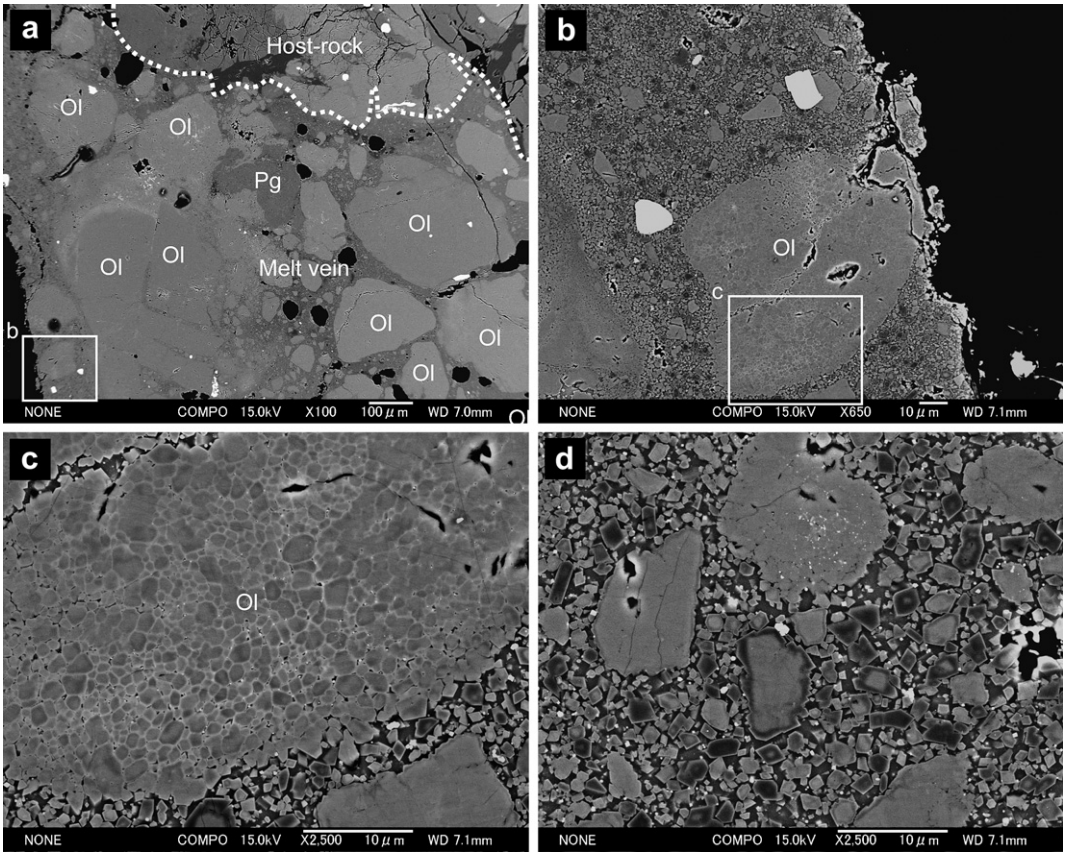

Fig. 2. Back-scattered electron images of the melt vein in lherzolitic shergottite Y984028. (a) Low-magnification image of the melt vein in lherzolitic shergottite Y984028. (b) Typical coarse fragment of olivine in the melt vein. (c) Enlargement of the area outlined by the square in (b). The coarse fragment shows a polycrystalline texture of euhedral to subhedral olivine crystals, especially along its margin, and several fine-grained chromite-like minerals exist in the interstices of the olivine crystals. (d) The matrix of the melt vein consists of fine-grained euhedral olivine crystals and interstitial glassy material; the fine-grained olivine shows several kinds of compositional zoning. Ol = olivine; Pg = pigeonite.

Table 2
Chemical compositions of the coarse fragments and matrix (composed of fine-grained olivine and interstitial glassy material) in the melt vein of lherzolitic shergottite Y984028.

	Olivine (fragment)		Olivine (matrix)		Pigeonite (fragment)		Maskelynite (fragment)		Glass (matrix)	
n	15		3		4		4		2	
Chemical composition (wt%)										
	av.	s.d.	av.	s.d.	av.	s.d.	av.	s.d.	av.	s.d.
SiO_2	37.35	0.14	38.08	0.59	53.29	0.12	55.52	1.48	51.85	0.60
TiO_2	b.d.	–	b.d.	–	0.51	0.06	n.d.	–	0.20	<0.01
Al_2O_3	b.d.	–	b.d.	–	1.15	0.15	26.61	1.23	20.43	0.15
Cr_2O_3	n.d.	–	n.d.	–	0.45	0.06	n.d.	–	b.d.	–
FeO	27.94	0.50	26.73	3.10	16.78	0.57	0.98	0.18	8.96	1.14
MnO	0.57	0.04	0.58	0.14	0.61	0.02	n.d.	–	0.25	0.01
NiO	b.d.	–	b.d.	–	n.d.	–	n.d.	–	n.d.	–
MgO	35.07	0.42	35.55	2.82	22.44	0.90	n.d.	–	6.00	0.39
CaO	0.22	0.04	0.26	0.06	5.32	1.40	8.34	0.83	8.93	0.33
Na_2O	n.d.	–	n.d.	–	0.10	0.02	6.30	0.42	3.34	0.47
K_2O	n.d.	–	n.d.	–	b.d.	–	0.29	0.09	0.12	0.01
Total	101.16	0.47	101.20	0.30	100.64	0.37	98.03	0.63	100.11	1.34
Cation formula										
Si	0.989	0.003	1.000	0.002	1.953	0.002	2.551	0.064		
Ti	–	–	–	–	0.014	0.002	–	–		
Al	–	–	–	–	0.050	0.006	1.441	0.068		
Cr	–	–	–	–	0.013	0.002	–	–		
Fe^{2+}	0.619	0.012	0.588	0.078	0.514	0.017	0.038	0.007		
Mn	0.013	0.001	0.013	0.003	0.019	0.001	–	–		
Ni	–	–	–	–	–	–	–	–		
Mg	1.384	0.012	1.391	0.085	1.226	0.050	–	–		
Ca	0.006	0.001	0.007	0.002	0.209	0.055	0.411	0.041		
Na	–	–	–	–	0.007	0.002	0.561	0.038		
K	–	–	–	–	–	–	0.017	0.005		
Total	3.011	0.003	3.000	0.002	4.005	0.004	5.018	0.014		
Oxygen	4		4		6		8			
Molecular proportions										
Fo	69	1	70	4	En 63	2	Ab 57	4		
Fa	31	1	30	4	Fs 26	1	An 42	4		
					Wo 11	3	Or 2	1		

Key: *n* = number of analyses; av. = average chemical composition; s.d. = standard deviation of analyses (1σ); b.d. = below the detection limit; n.d. = not determined.
Detection limits (in wt%): $TiO_2 = 0.02$, $Al_2O_3 = 0.02$, and NiO = 0.07 for olivine; $K_2O = 0.01$ for augite and pigeonite; $Cr_2O_3 = 0.1$ for chromite. All iron is assumed to be ferrous.

The matrix of the melt vein consists of fine-grained olivine (Fo_{67-75}) and interstitial glassy material (Fig. 2d and Table 2). The fine-grained olivines (~5 μm in diameter) are typically idiomorphic, and BSE images indicate the presence of several kinds of compositional zoning (Fig. 2d), mainly defined by variations in the Mg/Fe ratio. The nature of the compositional zoning differs from grain to grain, and we could recognize two types of pattern in the BSE images (Fig. 2d): (1) oscillatory zoning comprising Fe-rich cores, surrounding Mg-rich material, and finally Fe-rich rims; and (2) normal zoning comprising Mg-rich cores and Fe-rich rims. The interstices of the fine-grained olivine grains are filled with glassy material (Fig. 2d) of basaltic composition (Table 2).

4. Discussion

4.1. Comparison of Y984028 with other lherzolitic shergottites

Lherzolitic shergottites typically display two distinctive and contrasting petrographic textures: poikilitic and non-poikilitic. The poikilitic texture consists of large pyroxene oikocrysts enclosing subhedral olivine and euhedral chromite. The non-poikilitic texture

consists of a framework of olivine and minor pyroxene, with interstitial plagioclase (e.g., Harvey et al., 1993). In contrast to most lherzolitic shergottites, the Y984028 studied here exhibits only a non-poikilitic texture, possibly because the chip is small in size and is not a representative sample. The mineralogy and chemical compositions of the constituent phases in Y984028 are similar to those of other lherzolitic shergottites (e.g., Harvey et al., 1993; McSween and Treiman, 1998; Nyquist et al., 2001; Mikouchi and Kurihara, 2008). This finding suggests that Y980428 was a cumulate with a similar crystallization history and parental magma to those of other lherzolitic shergottites.

Mikouchi and Kurihara (2008) summarized the data on compositional variations of olivine in lherzolitic shergottites. The authors proposed a stratigraphic model for the igneous body from which lherzolitic shergottites originate, with the chemical composition of the olivine simply related to the depth of origin within the parental igneous body. The olivine (Fo_{67-69}) in Y984028 is almost identical in chemistry with the olivine in non-poikilitic areas of lherzolitic shergottites Y000027, Y000047, and Y000097 (Mikouchi and Kurihara, 2008). Therefore, Y984028 and these other lherzolitic shergottites may all have originated from a similar petrologic environment and parental block.

Previous studies have noted the abundance of shock features in lherzolitic shergottites (e.g., McSween and Treiman, 1998; Nyquist et al., 2001), and the shock metamorphic features of Y984028, such as irregular fractures in olivine and pyroxene, shock-induced twin-lamellae in pyroxene, and the complete conversion of plagioclase to maskelynite, are similar to those of other lherzolitic shergottites.

4.2. Comparison of the melt vein of Y984028 with melt veins/pockets in other lherzolitic shergottites

The melt vein in Y984028, studied here, contains rounded fragments of coarse-grained unzoned olivine, fine-grained zoned olivine, and interstitial glassy material (Fig. 2). The petrography of the melt vein is almost identical to that of the melt vein in Y000027, and in both, only euhedral zoned olivine crystals are present as the matrix of the veins (Mikouchi and Kurihara, 2008). However, the melt veins/pockets of other lherzolitic shergottites such as Allan Hills (ALH) 77005 and North West Africa (NWA) 1950 contain several textural types of olivine in their matrix, including dendritic, skeletal, and hollow (hopper) crystals, as well as euhedral ones (McSween et al., 1979; Walton and Herd, 2007a; Mikouchi and Kurihara, 2008).

The differences in olivine morphology in these various melt veins and melt pockets are related to differences in initial temperature and the cooling rates of the melt veins and pockets. Walton and Herd (2007b) conducted a series of crystallization experiments on synthetic glass that matched the bulk composition of a melt pocket in ALH 77005 lherzolitic shergottite. The starting temperature of the experiments varied from superliquidus, liquidus, and subliquidus temperatures, and each run was then cooled at rates of 10, 500, or 1000 °C/h. Based on the variety of olivine morphologies, which depended on the experimental conditions, the authors concluded that the melt pocket in ALH 77005 had cooled at a rate of 500–1000 °C/h, and that there was a gradient in the initial temperature of the melt from 1510–1520 °C at the center to 1460–1500 °C at the edge of the melt pocket. Applying their experimental results to the present case, the melt vein in Y984028 probably had an initial temperature of 1460–1500 °C, and then cooled at a rate of 10–500 °C/h, resulting in the crystallization of equant, euhedral olivine crystals, as observed in the Y984028 melt vein (Walton and Herd, 2007b).

However, the origin of the melt vein is unclear. Although there is clear evidence for shock metamorphism in Y984028, such as the complete conversion of plagioclase to maskelynite, we could not find any high-pressure phase in the melt vein. We might consider, therefore, two possibilities for the origin of the melt vein: shock-induced formation (*in situ* melting or injection of a shock-induced melt) or injection of a magmatic melt.

4.3. Polycrystalline olivine in the melt vein

Some coarse olivine fragments in the melt vein consist of polycrystalline fine-grained euhedral to subhedral olivine (Fig. 2c). This may be the product of the following processes. First, coarse olivine fragments from the host-rock were entrained in the melt and broken into many smaller olivine blocks due to shock-induced fragmentation and/or recrystallization. Subsequently, some of these smaller blocks formed coarse fragments by sticking to one another, in a process similar to sintering. The proposed sintering process is supported by the observation that tiny bright crystallites, probably chromite, are regularly found in the interstices of the fine-grained olivine crystals (Fig. 2c).

Alternative interpretation is that the euhedral, zoned olivine crystals in the matrix of the melt vein (Fig. 2d), which were crystallized from the melt, could have aggregated by a process of sintering to form the coarse

olivine fragments. In such a case, one would expect the olivine crystals making up the coarse fragments to display a variety of zoning patterns and chemical compositions, similar to those seen in the matrix of the melt vein (Fig. 2d). However, this is not the case, and all the crystals in a single polycrystalline fragment typically have similar zoning patterns and chemical compositions (Fig. 2c). This could be explained if the sintering process occurred at some other location, where only olivine crystals with a uniform zoning pattern and chemical composition were crystallized. The melt injected into Y984028 may then have picked up a variety of crystals and coarse fragments from several locations during the course of its flow.

4.4. Chemical zoning of the fine-grained olivine in the melt vein

The fine-grained olivines in the melt pockets of lherzolitic shergottites ALH 77005 and NWA 1950 show compositional zoning, with Mg-rich cores and Fe-rich rims (Walton and Herd, 2007a). In each melt pocket of these meteorites, the zoning patterns and chemical compositions of olivine crystals seem to be uniform. Similar zoning patterns and compositions were also synthesized in the crystallization experiments of Walton and Herd (2007b), and such a simple pattern of zoning is easily explained in terms of a change from a Mg-rich to an Fe-rich melt during the crystallization of olivine. However, in the case of the melt vein in Y984028, the fine-grained olivine crystals show several different zoning patterns and chemical compositions (Fig. 2d).

The observed two-dimensional zoning pattern of a crystal represents just one of many cross-sections through the three-dimensional crystal. Thus, even if in reality there was only one consistent pattern of zoning, several apparent zoning patterns may be observed as a consequence of the particular cut directions (e.g., an apparent normal zoning pattern could be formed by cutting an oscillatory-zoned grain along an off-center plane). However, the significant differences in chemical compositions, as observed in the Mg-rich layers of some olivine crystals, are difficult to explain by such an artifact as the cutting direction (Fig. 2d). In addition, the oscillatory zoning is difficult to explain by a simple compositional change of melt during crystallization.

The implication, therefore, is that the fine-grained olivine crystals in the matrix of the melt vein of Y984028 represent several crystallization environments and histories. For example, the oscillatory zoning could result from the following steps: (1) crystallization of Fe-rich olivine from an Fe-rich melt, (2) change in the melt composition to a more Mg-rich one due to melting of Mg-rich material, (3) growth of a Mg-rich layer from the Mg-rich melt, and (4) growth of the Fe-rich outermost rim due to a change in melt composition to an Fe-rich one during crystallization of olivine. Step (1) could also be explained by the existence of Fe-rich olivine fragments, formed by fragmentation and/or recrystallization of the host olivine, before crystallization of the vein melt. The normal zoning pattern comprising a very Mg-rich core and a Fe-rich rim may result from the crystallization of a Mg-rich melt, locally formed in the vein by the melting of Mg-rich minerals. Or, mixing of different melt containing different olivine crystals might also be possible.

5. Conclusions

We have investigated a chip of the lherzolitic shergottite Y984028, which contains a melt vein, with the aid of an FEG-SEM, an EPMA, and a laser micro-Raman spectrometer, yielding the following conclusions.

(1) Y984028 displays only non-poikilitic textures, but otherwise its petrography, mineralogy, and chemical composition are similar to those of other lherzolitic shergottites.
(2) The chemical composition of olivine in the host shergottite is almost identical to that of olivine in non-poikilitic areas of other lherzolitic shergottites such as Y000027, Y000047, and Y000097. According to Mikouchi and Kurihara (2008), Y984028 could therefore have originated in a similar Martian setting to those other lherzolitic shergottites.
(3) The melt vein in Y984028 is up to 1.5 mm wide, and it consists of rounded coarse fragments (mainly olivine), euhedral fine-grained olivine, and interstitial glassy material. These features are almost identical to those of the melt vein in lherzolitic shergottite Y000027 (Mikouchi and Kurihara, 2008).
(4) Some of the coarse fragments consist of a polycrystalline aggregate of fine-grained euhedral to subhedral olivine crystals. Possible interpretations include processes of shock-induced fragmentation and/or recrystallization of the host olivine, and aggregation by a sintering-like process. A similar process involving fine-grained liquidus olivine crystallized from the melt may also be possible.
(5) The fine-grained olivine crystals in the matrix of the vein exhibit several types of compositional zoning, including Fe–Mg–Fe oscillatory patterns. The

implication is that the fine-grained olivine crystals in the melt vein of Y984028 represent a complicated crystallization environments and histories.

Acknowledgments

We appreciate the opportunity provided by the National Institute of Polar Research for us to study the chip sample from Y984028. We thank Prof. A. El Goresy for his helpful discussion and encouragement. An anonymous reviewer is acknowledged for constructive comments that improved an early version of the manuscript. S. O. is supported by a JSPS Research Fellowship for Young Scientists. E. O. was partly supported by Grants-in-aid for Scientific Research (Nos. 18654091 and 18184009) from the Ministry of Education, Culture, Sports, Science, and Technology (MEXT), Japan, and the study was conducted as a part of the Tohoku University Global COE program "Global Education and Research Center for Earth and Planetary Dynamics".

References

Akaogi, M., Haraguchi, M., Nakanishi, K., Ajiro, H., Kojitani, H., 2010. High-pressure phase relations in the system $CaAl_4Si_2O_{11}$–$NaAl_3Si_3O_{11}$ with implication for Na-rich CAS phase in shocked Martian meteorites. Earth Planet. Sci. Lett. 289, 503–508.

Bogard, D.D., Johnson, P., 1983. Martian gases in Antarctic meteorite? Science 221, 651–654.

Clayton, R.N., Mayeda, T.K., 1996. Oxygen isotope studies of achondrites. Geochim. Cosmochim. Acta 60, 1999–2017.

Droop, G.T.R., 1987. A general equation for estimating Fe^{3+} concentrations in ferromagnesian silicates and oxides from microprobe analyses, using stoichiometric criteria. Mineral. Mag. 51, 431–435.

El Goresy, A., 2009. Shock-induced melting of maskelynite and the high-pressure mineral inventory of shergottites: implications to evaluation of the shock history of Martian meteorites. Eos Trans. AGU 90 (52), Fall Meet. Suppl., Abstract MR12A–03.

Harvey, R.P., Wadhwa, M., McSween Jr., H.Y., Crozaz, G., 1993. Petrography, mineral chemistry, and petrogenesis of Antarctic shergottite LEW88516. Geochim. Cosmochim. Acta 57, 4769–4783.

Imae, N., Ikeda, Y., 2010. High-pressure polymorphs of magnesian orthopyroxene from a shock vein in the Yamato-000047 lherzolitic shergottite. Meteorit. Planet. Sci. 45, 43–54.

Marti, K., Kim, J.S., Thakur, A.N., McCoy, T.J., Keil, K., 1995. Signatures of the Martian atmosphere in glass of the Zagami meteorite. Science 267, 1981–1984.

McSween Jr., H.Y., 1994. What we have learned about Mars from SNC meteorites. Meteoritics 29, 757–779.

McSween Jr., H.Y., Taylor, L.A., Stolper, E.M., 1979. Allan Hills 77005: a new meteorite type found in Antarctica. Science 204, 1201–1203.

McSween Jr., H.Y., Treiman, A.H., 1998. Martian meteorites. In: Papike, J.J. (Ed.), Planetary Materials. Mineralogical Society of America, Washington D.C., pp. 6-1–6-53.

Mikouchi, K., Kurihara, T., 2008. Mineralogy and petrology of paired lherzolitic shergottites Yamato 000027, Yamato 000047, and Yamato 000097: another fragment from a Martian "lherzolite" block. Polar Sci. 2, 175–194.

Nyquist, L.E., Bogard, D.D., Shih, C.-Y., Greshake, A., Stöffler, D., Eugster, O., 2001. Ages and geologic histories of Martian meteorites. Space Sci. Rev. 96, 105–164.

Walton, E.L., Herd, C.D.K., 2007a. Localized shock melting in lherzolitic shergottite Northwest Africa 1950: comparison with Allan Hills 77005. Meteorit. Planet. Sci. 42, 63–80.

Walton, E.L., Herd, C.D.K., 2007b. Dynamic crystallization of shock melts in Allan Hills 77005: implications for melt pocket formation in Martian meteorites. Geochim. Cosmochim. Acta 71, 5267–5285.

NiPR
National Institute of Polar Research

INTERNATIONAL POLAR YEAR 2007-2008